

Using X-Ray Imaging Model To Improve Guidewire Detection

Tomislav Petković and Sven Lončarić

University Of Zagreb, Faculty of Electrical Engineering and computing, Unska 3, Zagreb, Croatia

Email: {tomislav.petkovic,jr,sven.loncaric}@fer.hr

Abstract—Guidewire segmentation is the first step in producing automated tracking system to aid the surgeon during interventions. Most of the currently proposed methods for guidewire detection do not take into account X-ray imaging model and thus perform sub-optimally. We describe a simple imaging model and show how line detection technique based on the eigneanalysis of the Hessian matrix can be adapted to the model. Such adaptation improves detection results and allows application for a wider range of input images. Furthermore, we show how to choose an optimal set of parameters for the detection thus making the method fully automated.

Keywords—guidewire detection; multiplicative imaging; x-ray imaging.

I. INTRODUCTION

Minimally invasive endovascular intervention is the preferred treatment method for various vascular diseases. During such intervention guidewires are introduced into the cardiovascular system and must be navigated to a point of interest, usually a pathology. Accurate positioning and guidance of the guidewire is important and is one of the prerequisites for the successful procedure. The first step in constructing an automatic guide wire tracking system is guidewire segmentation.

We assume that X-ray imaging modality yields a 2D image where the guidewire is visible as a thin dark line. The actual imaging geometry is not of interest as the problem we discuss is limited to 2D segmentation. So we seek to segment the guidewire in a fluoroscopic image where it appears as a thin almost invisible line (Fig. 1). For this task any of the existing and well understood line or ridge detectors can be chosen.

Robust almost optimal line and ridge detectors are described by Steger [1] and Lindeberg [2]. Both are based on the analysis of the eigenvalues and eigenvectors of the Hessian matrix at preselected scale(s). Those approaches were extended to biomedical imaging applications in several studies: by Frangi et al. in [3] who define a vesselness measure that is based on the eigenvalues of the Hessian matrix to be used for extraction of line-like or tube-like structures, and by Baert et al. [4] and Walsum et al. [5] who apply it to the guidewire tracking problem. Other line detection approaches are based on families of rotated and steerable filters, but those are slightly more computationally expensive while the results are comparable to the Hessian based methods. A comparison of methods is given by Bismuth et al. [6] where the Hessian based method is found to be overall the fastest one while yielding results comparable to other techniques.



Fig. 1: A fluoroscopic input image. Guidewire can be seen in the lower right part of the image as a thin black line making one loop and then continuing toward the center of the image.

However, most of the aforementioned research does not take into account the physics of X-ray imaging. Unlike optical imaging where reflective radiation is measured, in X-ray imaging transmitted radiation is measured. This affects obtained image in a sense that every object on the ray path contributes to the observed intensity. For guidewire detection this results in a varying contrast along the line thus requiring that any applied line detection technique be made *locally adaptive*. Here, we present a new approach to guidewire detection, which is locally adaptive and based on the underlying physics of X-ray imaging.

This article is organized as follows: in Section II we describe simple X-ray imaging model, in Section III we review the Hessian eigneanalysis line segmentation methods and show how they can be adopted to the multiplicative imaging model. Results and discussion are given in Sections IV and V. We conclude in Section VI.

II. SIMPLE X-RAY IMAGING MODEL

Before discussing the adaptation strategy of the line segmentation algorithm a brief review of the X-ray imaging modality will be presented. The image formation model presented below is simplified, but is sufficient for developing a robust and fast guidewire segmentation algorithm.

X-rays produced by the radiation source are directed onto the detector with the patient placed in between. If a homogeneous isotropic object is placed on the ray path produced and measured radiation intensities can be related as $I = I_0 e^{-\mu d}$, where μ is linear attenuation coefficient and d is thickness of

the material [7]. A material with thickness d and coefficient μ changes observed intensity by a *multiplicative* factor of $e^{-\mu d}$.

When the patient is observed we should allow for multiple attenuation coefficients so

$$I = I_0 \exp\left(-\sum_i \mu_i d_i\right) \quad (1)$$

Equation (1) holds for pixels where the guidewire is absent, where $-\sum_i \mu_i d_i$ is the total attenuation coefficient associated with the patient (or background). However, when the guidewire is present we have additional multiplicative factor so

$$I = I_0 \exp\left(-\sum_i \mu_i d_i\right) \exp(-\mu_{\text{gw}} d_{\text{gw}}), \quad (2)$$

where the μ_{gw} is the attenuation coefficient associated with the guidewire. Let γ be the multiplicative term $\exp(-\mu_{\text{gw}} d_{\text{gw}})$. Equation (2) presents a model for the image acquisition under the assumption that the guidewire is thin when compared to the total tissue thickness, i.e. $d_{\text{gw}} \ll \sum_i d_i$.

III. GUIDEWIRE SEGMENTATION

As the imaging model is multiplicative line detection techniques must be adopted to the model. We focus solely on the Hessian matrix eigenanalysis based techniques as they have proven to be one of the most robust ones [6].

A. Hessian Matrix Eigenanalysis

For line enhancement filtering, as described in [1], [2], the second derivatives are needed. Convolution with the Gaussian is almost always combined with the second derivative operation in order to tune the filter response to the specific line width and to reduce undesirable effects caused by noise.

To find the Hessian matrix \mathcal{H} for image $I(i, j)$ at scale σ we compute

$$\mathcal{H}[G_\sigma(i, j) ** I(i, j)] = \mathcal{H}[G_\sigma(i, j)] ** I(i, j), \quad (3)$$

where $G_\sigma(i, j) = \frac{1}{\sigma_i \sqrt{2\pi}} \exp(-\frac{i^2}{2\sigma_i^2}) \frac{1}{\sigma_j \sqrt{2\pi}} \exp(-\frac{j^2}{2\sigma_j^2})$. From (3) we obtain 2×2 Hessian matrix for each pixel.

Justification for the line detection procedure is given by noting that (3) can be regarded as template matching. For the dark guidewire on bright background (usual setup) the convolution result in the center of the guidewire would be positive. Otherwise, for white guidewire on dark background, it would be negative.

The result of (3) for discrete image is again 2×2 matrix $\mathbf{H} = \begin{bmatrix} L_{xx} & L_{xy} \\ L_{yx} & L_{yy} \end{bmatrix}$, where L_{xx} , L_{xy} and L_{yy} are results of convolution with the sampled Gaussian (or first or second derivative) at scale σ . Eigenvalues of the matrix \mathbf{H} are analyzed to extract the principal directions in which the second order structure can be decomposed. Such analysis yields the directions of the smallest curvature (along the ridge) and extracts two invariant orthonormal directions (determined up to scaling if the matrix has full rank) when the image is mapped by the Hessian matrix that can be thought of as an ellipse aligned along the line like structure [3], [2]. If the eigenvalues λ_k are ordered so $|\lambda_2| >$

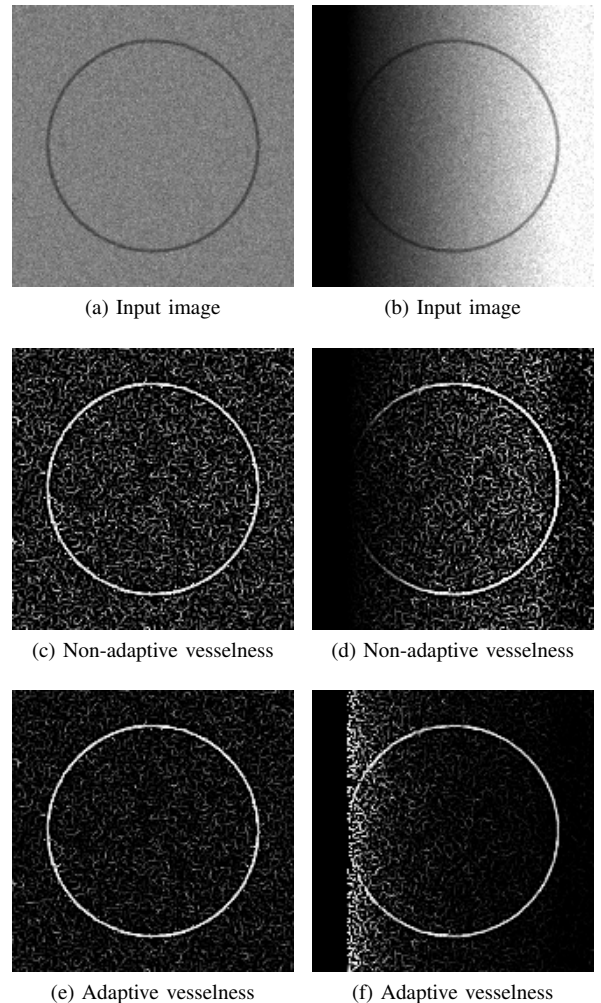


Fig. 2: Example of detection results for simulated input with uniform (a) and non-uniform (b) background. (c) and (d) show vesselness maps obtained with globally set parameters. (e) and (f) are locally adapted vesselness maps.

$|\lambda_1|$ an elongated line like structure would be associated with the elongated ellipse characterized by $|\lambda_2| \gg |\lambda_1|$.

Eigenanalysis is usually done at different scales σ . For guidewire tracking the choice of σ does not present a problem as the wire diameter is known in advance thus making analysis at a fixed scale corresponding to the diameter.

B. Line Model

Steger [1] discusses 1D model bar-shaped line profile as the simple line model for reflective images. For 1D case intensity profile $I(x)$ of a line with width w and contrast h is given by

$$I(x) = \begin{cases} h, & |x| < \frac{w}{2} \\ 0, & \text{otherwise} \end{cases}. \quad (4)$$

For 2D case profile (4) is extended so $I(i, j)$ is equal to 1D profile when evaluated along the direction perpendicular to the local line orientation while the 1D profile is repeated in

orthogonal direction. The optimal scale for this model is $\sigma = \frac{w}{2\sqrt{3}}$ [1].

Model (4) is not directly applicable to X-ray imaging as it is not multiplicative. Line contrast h is now not an absolute value, but a relative one. The multiplicative factor associated with the wire is γ so line contrast becomes relative value depending on the background intensity $b(i, j)$. 1D profile along the direction orthogonal to the line direction is now

$$I(x) = \begin{cases} \gamma b(x), & |x| < \frac{w}{2} \\ b(x), & \text{otherwise} \end{cases}. \quad (5)$$

Under the assumption of relatively constant background (the background must have stable values in the square patch of the size 3σ around the line center point) maximal possible eigenvalue value associated with this model is $L_{xx, \max} = b(i, j)(1 - \gamma) \frac{2\sqrt{3}}{\sigma\sqrt{2\pi}} e^{-3/2}$. As we cannot measure the original background intensity $b(i, j)$ we replace $b(i, j)$ by $I(i, j)/\gamma$, where $I(i, j)$ is measured intensity, so

$$L_{xx, \max} = I(i, j) \frac{1 - \gamma}{\gamma} \frac{2\sqrt{3}}{\sigma\sqrt{2\pi}} e^{-3/2}. \quad (6)$$

The line position in the image is obtained by thresholding the larger eigenvalue. The threshold must be selected based on the value of (6).

C. Adapting The Vesselness Measure

To classify pixels as belonging to the guidewire the vesselness map is computed. Vesselness is a function that maps extracted features into the probability like estimate enabling easier interpretation [3]. It is computed as

$$\mathcal{V}(\sigma) = \exp\left(-\frac{\lambda_1^2}{\lambda_2^2} \frac{1}{2\alpha^2}\right) \left(1 - \exp\left(-\frac{\lambda_1^2 + \lambda_2^2}{2\beta^2}\right)\right) \quad (7)$$

where α and β are parameters that control the sensitivity. If we want to detect only dark lines the measure can be set to zero for $\lambda_2 < 0$.

As the maximal absolute expected eigenvalue is determined by (6) the optimal parameters α and β for the vesselness map computation can be chosen. Those parameters must be chosen *independently for each input pixel* thus making the method locally adaptive.

Parameter α is dependent on the guidewire attenuation coefficient as it controls the contribution of the ratio $\frac{\lambda_1}{\lambda_2}$. Furthermore, the ratio is independent of the input image amplitude scaling. As $|\lambda_2| > |\lambda_1|$ the ratio is always less than 1 with $\alpha \in \langle 0, \frac{1}{2\ln 2} \rangle$. For the choice of $\alpha = \frac{1}{2\ln 2}$ the response for a perfect blob-like structure (ratio is one) is exactly the minimal possible value of the term. The chosen α should be closer to $\frac{1}{2\ln 2}$ then zero, as lower values for α tend to make short but locally highly curved lines impossible to detect. The limit value of $\frac{1}{2\ln 2}$ is optimal so term $\exp(-\frac{1}{2\alpha^2}(\frac{\lambda_1}{\lambda_2})^2)$ can attain values in the interval $[\frac{1}{2}, 1]$.

Parameter β is controlling the contribution of the sum of squares $\lambda_1^2 + \lambda_2^2$. For the line-like structures the sum of squares will be approximately λ_2^2 , with the value of $|\lambda_2|$ given by (6).

To choose the value of parameter β we must know the scale σ and the expected attenuation γ . Once those are known (6) yields required β . For example, if for attenuation factor of γ we want the second term in (7) to obtain value x we choose

$$\beta(x) = I(i, j) \frac{1 - \gamma}{\gamma} \frac{2\sqrt{3}}{\sigma\sqrt{2\pi}} e^{-3/2} \frac{1}{\sqrt{-2\ln(1-x)}}.$$

Such choice of β guarantees detection of all line-like structures with smaller attenuation γ , so to choose β we must know the lowest attenuation coefficient we want to detect.

Based on the discussion so far if we want to detect the guidewire with the diameter d and attenuation γ the optimal parameters for the vesselness map are $\sigma = \frac{w}{2\sqrt{3}}$, $\alpha = \frac{1}{2\ln 2}$ and $\beta = I(i, j) \frac{1 - \gamma}{\gamma} \frac{2\sqrt{3}}{\sigma\sqrt{2\pi}} e^{-3/2} \frac{1}{\sqrt{-2\ln(4)}}$.

IV. RESULTS

For quantitative evaluation of the proposed detection method we use synthetic images.

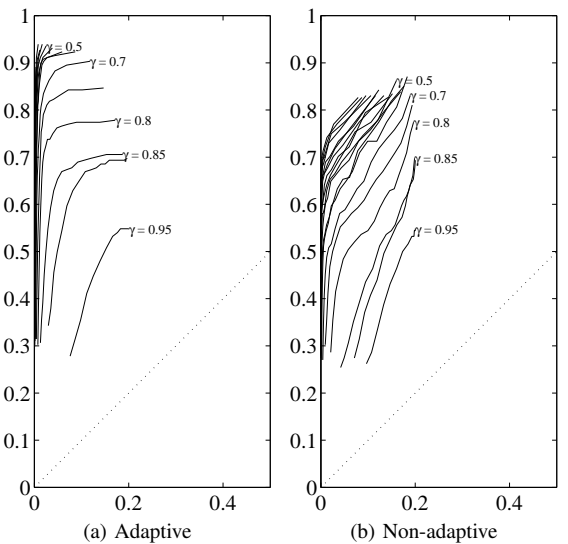


Fig. 3: ROC curves for various guidewire attenuation factors.

To generate the synthetic images we use the multiplicative model where ideal background value $b(i, j)$ is multiplied by factor c that is a combination of the wire attenuation γ and the pixel area covered by the simulated wire. To make evaluation more realistic we degrade the synthetic images with image dependent Poissonian noise with the intensity set to $cb(i, j)$. The resulting pixel values are quantized to 8 bits.

As the constant background is not a realistic assumption we evaluate the method on images showing a circular guidewire where the background linearly changes from 0 to 255 (Fig. 2b). Such background clearly illustrates effects we can expect when the method is used on real-world images.

To quantitatively evaluate the proposed method we compute the ROC curves (Fig. 3) for the proposed adaptive line detector (Fig. 3a) and for the standard non-adaptive line detector (Fig. 3b), for a wide range of attenuation coefficients γ . Note

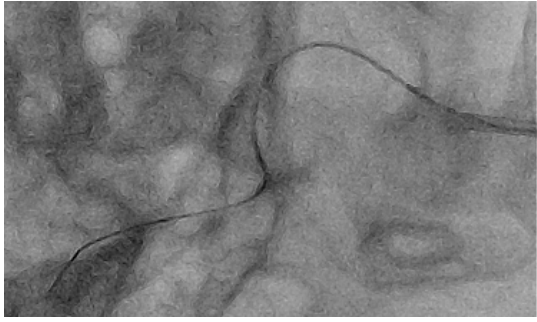


Fig. 4: Input x-ray image.

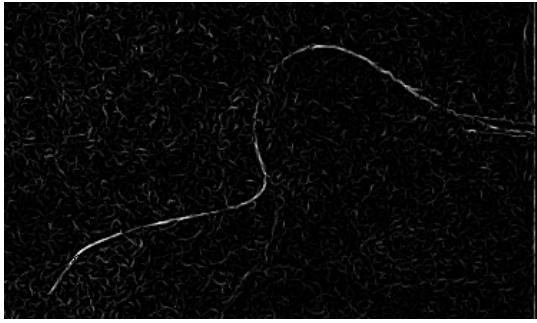


Fig. 5: Non-adaptive vesselness map.

that the starting γ of 0.95 corresponds to contrast-to-noise ratio (CNR) of about 0.6. Note the shift of the ROC curves.

To show qualitative difference on real-world images we give one example. Typical x-ray image for neuroendovascular intervention is shown in Fig. 4. Guidewire is visible and extends starting from the right side toward left bottom of the image. Fig. 5 shows non-adaptive vesselness while fig. 6 shows adaptive vesselness with annotated areas of interest. Note there is no reduction in brightness for anatomical landmark (A), but with slight drawback being increased vesselness value for local line-like structures located in darker areas of the image (B). Overall background clutter is significantly reduced (C).

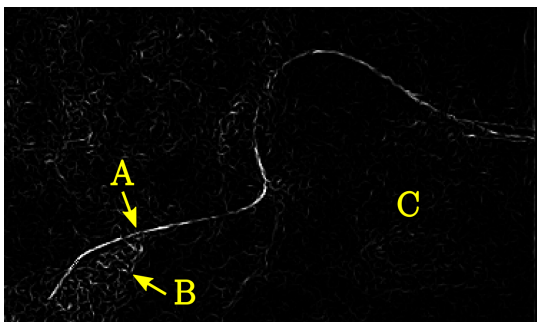


Fig. 6: Adaptive vesselness map with three areas of interest shown: A) reduced intensity decrease; B) stronger detection for local-line like structures on dark background; C) better suppression of background noise.

V. DISCUSSION

The proposed adaptive line detector extends the usability of the guidewire detection techniques. By comparing images in Fig. 2 for uniform (first column) and non-uniform (second column) backgrounds the vesselness map is more accurate when parameter β is locally adapted. Furthermore, by comparing images 2d and 2f it is clear that adaptive method can detect the guidewire more reliably in the case of varying contrast (compare the detection results on the left side as the background slowly descends towards zero). This is the most important effect of local adaptation as during the interventional procedures the guidewire will be superimposed on various anatomical landmarks that often affect the absolute contrast value thus making detection with a fixed (non-adaptive) set of parameters unfeasible.

VI. CONCLUSION

We have presented a new method for adaptive line detection that is specifically formulated for a multiplicative imaging model such as X-ray imaging. This has improved the segmentation results, especially when the guidewire is occluded by various anatomical landmarks such as bones.

In the field of biomedical imaging image data to be analyzed is almost always obtained in controlled conditions with imaging models and acquisition protocols known in advance. This fact should be of greater interest to researchers in the field of biomedical image processing and analysis as it usually enables construction of strict imaging model that can then be applied to enhance or adapt established methods thus making them better suited to the task at hand.

REFERENCES

- [1] C. Steger, "An unbiased detector of curvilinear structures," *Pattern Analysis and Machine Intelligence, IEEE Transactions on*, vol. 20, no. 2, pp. 113–125, Feb. 1998.
- [2] T. Lindeberg, "Edge detection and ridge detection with automatic scale selection," in *Computer Vision and Pattern Recognition, 1996. Proceedings CVPR '96, 1996 IEEE Computer Society Conference on*, Jun 1996, pp. 465–470.
- [3] A. F. Frangi, W. J. Niessen, K. L. Vincken, and M. A. Viergever, "Multiscale vessel enhancement filtering," in *MICCAI '98: Proceedings of the First International Conference on Medical Image Computing and Computer-Assisted Intervention*. London, UK: Springer-Verlag, 1998, pp. 130–137.
- [4] B. SAM, M. Viergever, and W. Niessen, "Guide-wire tracking during endovascular interventions," *Medical Imaging, IEEE Transactions on*, vol. 22, no. 8, pp. 965–972, Aug. 2003.
- [5] T. van Walsum, S. Baert, and W. Niessen, "Guide wire reconstruction and visualization in 3dra using monoplane fluoroscopic imaging," *Medical Imaging, IEEE Transactions on*, vol. 24, no. 5, pp. 612–623, May 2005.
- [6] V. Bismuth, L. Vancamberg, , and S. Gorges, "A comparison of line enhancement techniques: applications to guide-wire detection and respiratory motion tracking," in *Proc. SPIE*, vol. 7259. SPIE, Mar. 2009.
- [7] B. Hasegawa, *Physics of Medical X-Ray Imaging*, revision of 2nd edition ed. Medical Physics Publishing Corporation, 1987.